ÓPTICA PURA Y APLICADA
www.sedoptica.es

Type: RESEARCH PAPER
Section: Optical Metrology and Instrumentation

Optical behavior simulation of the divergence adapter elements in a Ronchi deflectometry configuration for convex surfaces

Simulación del comportamiento óptico de los elementos adaptadores de divergencia en una configuración de deflectometría Ronchi para superficies convexas

F. Gonzales,[1,*] J. Arasa[2]

1 Departamento de Ciencias, Sección Física, Pontificia Universidad Católica del Perú, San Miguel, Lima 32, Perú

2 Universitat Politècnica de Catalunya, Rambla Sant Nebridi 10, Terrassa 08222, Spain

(*) E-mail: fgonzales@pucp.edu.pe S: miembro de SEDOPTICA / SEDOPTICA member

Received: 18/02/2022 Accepted: 09/08/2022
DOI: 10.7149/OPA.55.3.55107

ABSTRACT:

The primary purpose of this article is to show the simulation of the optical behavior of the divergence adapter elements in the Ronchi deflectometry configuration to measure convex surfaces, which so far has not been reported in the literature. The use of divergence adapter elements is mandatory when Ronchi deflectometry is used to obtain the shape of a convex surface. Otherwise, light reflected by the surface cannot be collected into the measuring stage. Divergence adapters must be included in both arms of the Ronchi deflectometry configuration, keeping in mind that their optical behaviors affect the surface shape measurement. Before carrying out an experimental setup, we analyzed these elements' effects through an optical simulation of the selected Ronchi. From the analysis of the optical simulation, we can check the adequacy of the divergence adapter for the expected measuring range and required accuracy; the decision about its suitability has been taken by looking if the relations between slope and position at the apex of the convex surface was unequivocal. In this paper, we present the Ronchi configuration chosen to measure convex surfaces, the selected lenses for the divergence adapters, the thresholds linked to the sampler's elements, the optical simulation, and the criteria used to answer if the behavior of the divergence adapters is appropriated for the radii interval that we want to measure. Finally, a unique polynomial expression is proposed to transfer slope and position values from the sampling elements of the apex plane of the surface to be measured.

Keywords: Ronchi deflectometry, convex surfaces, divergence adapter, simulation, metrology.

REFERENCES AND LINKS / REFERENCIAS Y ENLACES

[1] V. Ronchi, "Due nuovi metodi per lo studio delle superficie e dei sistemi ottici," Nuovo Cim 26, 69–71 (1923).

[2] F. Jentzsch, ''Die Rastermethode: Ein Verfahren zur Demonstration und Messung der Spharischen Aberration,'' Phys. Z., 24, 66 (1928).

[3] G. Toraldo di Francia, ''La Prova dell'Aberrazione Cromatica con l'Interferometro a Reticolo,'' *Ottica*, 7, 302 (1942).

[4] I. Adachi, ''The Recent History of the Grating Interferometer and Its Applications,'' Atti. Fond. Giorgio Ronchi Contrib. 1st. Naz. Ottica, 17, 252–259 (1962).

[5] I. Adachi, ''Measurement of Transfer Function of the Ronchi Test,'' *Atti. Fond. Giorgio Ronchi Contrib. 1st. Naz. Ottica*, 17, 523–534 (1962).

 © Sociedad Española de Óptica

[6] V. Ronchi, "Forty Years of History of a Grating Interferometer," Appl. Opt. 3, 437-451 (1964).
[7] A. Cornejo and D. Malacara, "Ronchi test of aspherical surfaces, analysis, and accuracy," Appl. Opt. 9, 1897–1901 (1970).
[8] J. D. Briers and M. J. Cochrane, ''Ronchi Test Formulae 2: Practical Formulae and Experimental Verification,'' Opt. Laser Technol., 11, 245–257 (1979).
[9] A. Cornejo-Rodriguez, "Ronchi test," in *Optical Shop Testing*, 3rd ed., D. Malacara, ed. Wiley, New York. (2007).
[10] José Hernández Delgado, Zacarías Malacara-Hernández, Daniel Malacara-Doblado, Benito Vázquez Dorrío, and Daniel Malacara-Hernández "Local curvatures and its measurements of an optical surface or a wavefront: a review," Optical Engineering 61(5), 050901 (2022).
[11] Yusuke Saita, Daiki Shimoyama, Ryohei Takahashi, and Takanori Nomura, "Single-shot compressive hyperspectral imaging with dispersed and undispersed light using a generally available grating," Appl. Opt. 61, 1106-1111 (2022).
[12] Javier Salinas-Luna, FermIn-Solomon Granados-AgustIn, Alejandro Cornejo Rodriguez, Esteban A. Luna-Aguilar, Juan Jaime Sanchez-Escobar, Juan Manuel Hernández-Cid, "Ronchi test with variable-frequency rulings," Opt. Eng. 48(1) 013604 (2009).
[13] Sukmock Lee and Dae Wook Kim "Two-dimensional Fourier domain Ronchi ruling measurement using Talbot-based crossing point modeling," Optical Engineering 59(1), 014106 (2020).
[14] D. Malacara and A. Cornejo, "Null Ronchi Test for Aspherical Surfaces," Appl. Opt. 13, 1778-1780 (1974).
[15] A. C. Rodríguez., "Null Methods in Optical Testing," in Latin America Optics and Photonics Conference, OSA Technical Digest (online) (Optical Society of America, 2014), paper LF1B.1.
[16] D Aguirre-Aguirre, "Null Ronchi Gratings as a function of period," in J. Phys.: Conf. Ser. 605 012015, 2015.
[17] K. Omura and T. Yatagai, "Phase measuring Ronchi test," Appl. Opt. 27, 523-528 (1988).
[18] DS Wan and DT Lin, "Ronchi test and a new phase reduction algorithm," Appl. Opt. 29, 3255-3265 (1990).
[19] N. Acalá-Ochoa, M. Mora-González, and F. Mendoza, "Flatness measurement by a grazing Ronchi test," Opt. Express 11, 2177-2182 (2003).
[20] M. Mora-González and N. Acalá-Ochoa, "Sinusoidal liquid crystal display grating in the Ronchi test," Opt. Eng. 42(6), 1725–1729 (2003).
[21] A. Cordero-Dávila, J. González-García, C. I. Robledo-Sánchez, and I. Leal-Cabrera, "Local and global surface errors evaluation using Ronchi test, without both approximation and integration," Appl. Opt. 50, 4817-4823 (2011).
[22] J. A. Arriaga-Hernández and A. Jaramillo-Núñez, "Ronchi and Moiré patterns for testing spherical and aspherical surfaces using deflectometry," Appl. Opt. 57, 9963-9971 (2018).
[23] D.Malacara,"Geometrical Ronchi test of aspherical mirrors", App.Opt. 4(11) 1371-1373 (1965).
[24] A. Cornejo and A. Malacara, "Ronchi test of aspherical surfaces, analysis, and accuracy," Appl. Opt. 9, 1897–1901 (1970).
[25] J. Arasa, S. Royo, and C. Pizarro, "Toroidal surface profilometries through Ronchi deflectometry: constancy under rotation of the sample," in Applications of Photonic Technology, G. A. Lampropoulos, and R. A. Lessard, eds., Proc. SPIE 3491, 909–915 (1998).
[26] S. Royo, J. Arasa, and C. Pizarro, Profilometry of toroidal surfaces with an improved Ronchi test, Appl. Opt. 39, 5721-5731 (2000).
[27] Chun-Li Chang, Wen-Hong Wu, and Chun-Jen Chen "A study on an automatic Ronchi test system," Proc. SPIE 9217, Applications of Digital Image Processing XXXVII, 92172A (2014).
[28] R. Díaz-Uribe and M. Campos-García, "Null-screen testing of fast convex aspheric surfaces," Appl. Opt. 39, 2670-2677 (2000).
[29] F. Gonzales and J. Arasa, *Determinación del error inducido en los haces de muestreo y medida de un sistema de medida Ronchi para superficies convexas debido al uso de sistemas ópticos reales*, conference RIAO OPTILAS-MOPM 2019 conference (237-238), 23-27 September, (2019).

 © Sociedad Española de Óptica

[30] A. Moreno and J. Campos, "Revision of different optical metrology techniques," Opt. Pura Apl. 40 (3) 267-280 (2007).

1. Introduction

From the appearance of the Ronchi test to the present, optical metrology has used this measuring technique to evaluate optical reflective surfaces and measure aberrations of optical systems [1-10]. The interpretation of the Ronchi test can be geometrical [7,9,10], known as Ronchi deflectometry, or in a waveform [1,3,7,9,11], known as the Ronchi test; in the most common configuration, a periodic grating of transparent and dark stripes is used for sampling the wavefront. Through the years, the periodic grating has undergone many adaptations, from variations in its period [12,13] to its modification to perform a "null test" [14-16] or its implementation for phase displacement [17-20]. Usually, the Ronchi test has been applied to evaluate concave surfaces, whether spherical or aspherical [21-24], with and without rotational symmetry [25-27]. In the previous citations, the novelty focused on improvements in the shape of the grating, the use of algorithms and strategies to improve the measurement, the increase of the dynamic range, or the complexity in the sample's shapes, but not in the case where the sample is a convex surface [28].

According to current literature, the application of Ronchi deflectometry to measure convex surfaces has not been reported so far. Implementing a Ronchi deflectometry system that measures convex surfaces leads us to the compromise of implementing an optical system with divergence adapters [29], which are necessary to collect the light reflected on the convex surface being measured. For this reason, we need to study the behavior of divergence adapters.

The presence of the divergence adapter adds more complexity to the measurement process because the information obtained in the Ronchi plane and the slope measurement system needs to be transferred to the apex of the convex reflective surface that we want to measure (from now on, the apex), using the divergence adapter. In addition, the divergence adapter placed in the illumination arm affects the slopes of the rays that, coming from the light source, reaches the surface. In both cases, the aberrations introduced by the divergence adapter can be high enough to lose the unequivocal associations between position and slope, risking the measurement process not being carried out correctly.

To overcome this possible source of error, we obtained the optical behavior of the divergence adapter through its simulation before building a lab prototype, using OSLO™ (optical design software) in the same conditions we aim to use in the experimental setup. The simulation analysis has confirmed that the chosen lens group works correctly as a divergence adapter. The procedure to determine if a divergence adapter can be appropriately used in a Ronchi deflectometry arrangement to measure reflective convex surfaces can be written in a general way: "if two, or more, rays share the same position in the apex plane, the divergence adapter is not valid." However, the simulations and analysis need to be done for a specific configuration, and a threshold value is required to decide if two neighbor rays share or not the same position; that is to say, the answer is linked to the configuration and spatial resolution of the sampling.

For this reason, we introduce the selected configuration of the Ronchi measuring system and how the availability constraints and measurement requirements have led us to our selection. Once the selection is made, we proceed separately to do the optical simulation of each arm, illumination, and measurement. The obtained values and the available spatial resolution provide enough information to answer whether the divergence adapter is appropriate for the selected Ronchi configuration. This procedure, at minimum, must be done on the extreme values of the radii we wish to measure; it has also been applied at two intermediate radius values to ensure the quality of the selected configuration. For easier viewing and evaluating the divergence adapter's behaviors, we have fitted an odd fifth-order polynomial to the transfer functions of both arms for each radius value analyzed.

2. Selected Ronchi configuration

The introduction explains that when Ronchi deflectometry [25,26,30] is used to measure convex surfaces, the process becomes more complex [29] than a concave surface. Additional divergence adapters and lens sets are required to properly converge light onto the convex surface and collect reflected light, which is involved in the measurement process and the properties of these divergence adapters, depending on the

 © Sociedad Española de Óptica

selected Ronchi configuration. Since the placement and number of items may differ for each Ronchi configuration, we must explain our chosen configuration first.

The selected Ronchi configuration is designed to measure changes in the shape of reflective convex surfaces of curvature radii between 5 to 20 mm when an approximate initial value of those radii is known. The light source, see Fig. 1a) is monochromatic at 635 nm with a numerical aperture (from now on, NA) of 0.14 and an emitting diameter of 125 µm (Thorlabs LPS-635-FC) and acts like a quasi-punctual light. The illumination and measurement arms share their optical paths through a cube beam splitter 50/50 of 10x10x10 mm of glass N-BK7 (Edmund Optics 47121). And the sampling elements placed in the measurement arm are a custom-made Ronchi ruling, with a size of 20x20 mm and a frequency of 1mm-1 with dark stripes that cover half of the period and a monochrome CMOS sensor of 1280x1024 pixels with a pixel size of 5.2 µm (Thorlabs DCC1545M).

The sampling elements, both placed in the measurement arm, provide the threshold values for the divergence adapter analysis. The Ronchi ruling has been placed in front of the second unitary magnification system (S_2) and does not conjugate with the apex, covers a measuring field of 10 mm (approx.) and its frequency of 1 mm^{-1} allows to make ten samples. That is, it acts as a low-frequency Ronchi test whose resolution can be improved in the data processing stage using, for example, the phase-shifting technique. Let's consider that the accuracy in the position determination must be less than ten times better than the sampling period. We obtain a threshold value of 1/100 of the field size for the position determination, that is 0,01 mm in the Ronchi ruling plane.

Once the Ronchi ruling has sampled the positions in the measuring field, the corresponding slope values are obtained through the CMOS sensor. To get the slope values, the CMOS sensor must be placed in the focal plane of a lens that, working together, provides a correspondence between each CMOS sensor pixel and a slope value, see Fig. 1b). The achromatic doublet chosen to work with the CMOS sensor has an effective focal length (EFL) of 25 mm and an aperture of 12.5 mm (Edmund Optics 32311), and the assembly will be named, from now on, the slope measuring system (SMS). The SMS not only introduces a second threshold but also does design constraints on the selected Ronchi configuration. The shorter side of the sensor has a size of 5.3 mm (1024x5.2 µm), and with the achromatic doublet of 25 mm EFL, the SMS can cover an angular field of 12 degrees, ± 0.105 slope values or a numerical aperture of NA=0.105.

To take the maximum profit of the SMS measuring range, we need to spread the shadows of the Ronchi ruling along with all the sensor size. In this situation, the threshold for the position determination is directly transferred to the threshold for the slope determination, so it is also 1/100 of the measuring field of 7.2 arc minute or 0.0021 slope units or 10 pixels on the CMOS sensor. However, the SMS also constraints the design process because to maintain the numeric aperture for all the radius values that we aim to measure, two conditions must be met; the illumination arm must have the same value of numeric aperture, and the curvature center of the surfaces under test need to be permanently placed in the same position. Finally, although the SMS is not a component of the divergence adapter, both it and the cube beam splitter must be included in the simulations to obtain the optical behavior of the divergence adapter because they also introduce changes in the light path.

Once the threshold values and constraints are known, the design process can continue. The SMS fixed the maximum slope value (±0.105), and the rays must come into the SMS through its entrance pupil. To place it in an accessible position, the Ronchi ruling, we have added a unit magnification system (S_2), ELF 50 mm, and 12.5 mm of aperture (Edmund Optics 55272) that conjugates the entrance pupil of the SMS in a point near the cube beam splitter and allows to locate the Ronchi ruling in front of it, see Fig. 1a). S_2 is part of the divergence adapter placed in the measurement arm and plays a triple role, conjugates the entrance pupil of the SMS, maintains the numerical aperture, and allows an accessible place for the Ronchi ruling.

Following in the measurement arm, two more elements are found before reaching the surface under test; from now on, the surface, a cube beam splitter, and another unitary magnification system (S_1) with the exact optical specifications that S_2. The numerical aperture of the SMS and the size of the cube itself determine the placement of the beam splitter, while S_1 conjugates simultaneously the image of the entrance pupil of the SMS, done by S_2, and the light source at a point near the center of curvature of the surface. In this situation, see Fig. 1c), the incident and the reflected rays are close to the local normal, and the surface does not introduce relevant changes in the divergent values. The divergence adapter of the measuring arm is the system composed of S_1 and S_2. The simulation process must submit the cube beam splitter and the SMS to obtain the correct behavior.

 © Sociedad Española de Óptica

The measurement arm also determines all the elements of the illumination arm, see Fig. 1a) because they are shared through the beam splitter; in this way, the divergence adapter of the illumination arm is the element S_1, and the simulation process needs to introduce the cube beam splitter to obtain the correct behavior. Through its sampling elements, the measuring arm provides couples of value position-slope from the reflected light on the surface, and the illumination arm provides the slope value, at the previously selected positions, from the incident light. Although the illumination arm does not have any sampling element, the same threshold, 1/100 of the measuring field, must be applied at the relations position-slope for the incident light because if the aberrations of the illumination arm introduce equivocal associations between positions and slope, the further steps of the Ronchi measuring strategy will be wrong.

The Ronchi configuration selected provides the raw data of position-slope values to obtain the shape of the surface; the speed, repeatability, and accuracy of the measure are related, also to the measurement strategy applied.

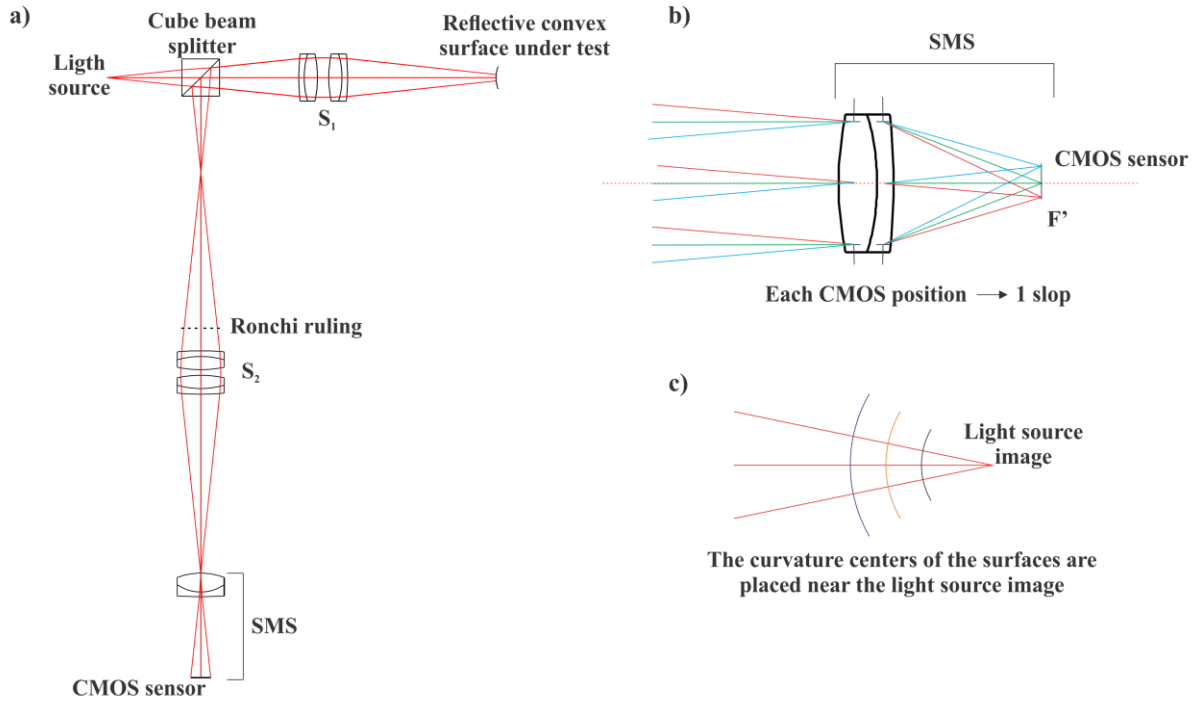

Fig. 1 Layout of the selected Ronchi configuration. a) The divergence adapter of the measuring arm is the system composed of S_1 and S_2, and the divergence adapter of the illumination arm is the element S_1. b) In the slope measuring system (SMS) scheme, the CMOS sensor is placed in the focal point; each sensor position is directly related to a slope value. c) To maintain the numerical aperture (NA), the image of the light source must be placed near the curvature center of the surfaces.

3. Optical simulations

As we have explained, checking the suitability of the divergence adapters in our Ronchi deflectometry design is necessary to perform the optical simulation for both arms separately. The simulation has been done for the extremal radius values that we aim to measure, 5 and 20 mm, and two extra intermediate values, 10 and 15 mm, to test the behavior in all ranges.

All simulations have been performed using OSLO™ software. Since we have selected a quasi-point monochromatic light source, we do not need to analyze both field and chromatic aberrations. The Ronchi measurement process needs to obtain three sets of raw data related to each other; two of them, the positions and the slope after the light is reflected from the surface, are obtained in the measurement arm, using the rule of Ronchi and SMS as sampling elements, respectively. The third set of data is the slopes of the incident light and is obtained using the relationship between the position and the slope in the lighting arm.

Our Ronchi configuration is focused on measuring convex reflective surfaces, so introducing divergence adapters affects the raw data values. To find out the behavior of each divergence adapter, we need to do the simulations optically disconnecting the two arms of the configuration, see Fig. 2. To do the simulations in the measurement arm, the surface must be skipped, and the light source must be placed in its center of

 © Sociedad Española de Óptica

curvature, see Fig. 2a); for the simulation in the illumination arm is only necessary to skip the surface, see Fig. 2b).

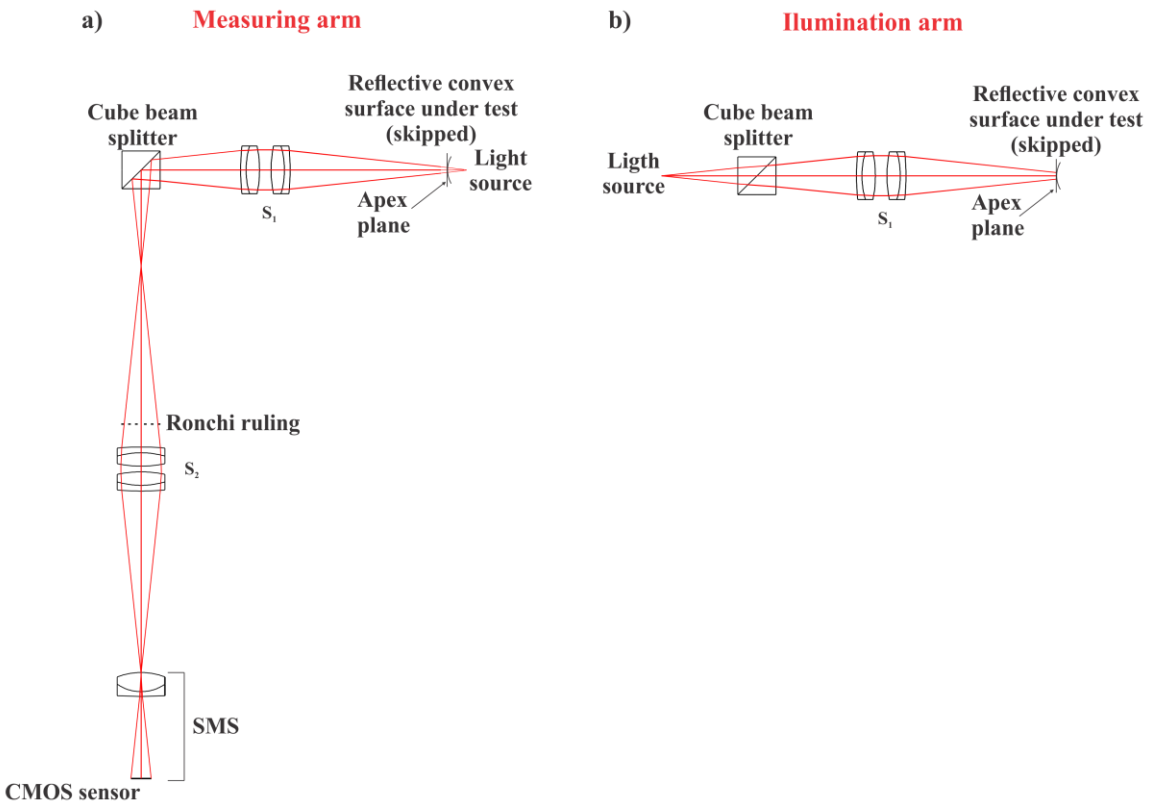

Fig. 2 Layout to simulate the behavior of the divergence adapters. a) In the measuring arm. b) In the illumination arm.

To analyze the behavior of the divergence adapter in the measurement arm, we need to obtain two relations: one between the position in the Ronchi ruling and the position at the apex and the other between the position in the CMOS sensor plane of the SMS and the slope in the apex. A graph representation of these relations for the selected radii (5, 10, 15, and 20 mm) is shown in Fig. 3. For easy treatment, a polynomial fit of each relationship has been done and shown in table 1.

The position and slope data used for the graphs shown in Fig. 3 and Fig. 4 have been extracted from the OSLO™ simulation. Simulation of the illumination arm was first performed (Fig. 2b), and 41 values of the position and slopes on the apex of the convex surfaces were obtained. Next, the system simulation was implemented up to the Ronchi ruling (Fig. 2a) to get the 41 position values on the Ronchi ruling. Finally, the measurement arm was simulated up to the image plane representing the CMOS sensor (Fig. 2a), obtaining the 41 values for the position in the SMS.

 © Sociedad Española de Óptica

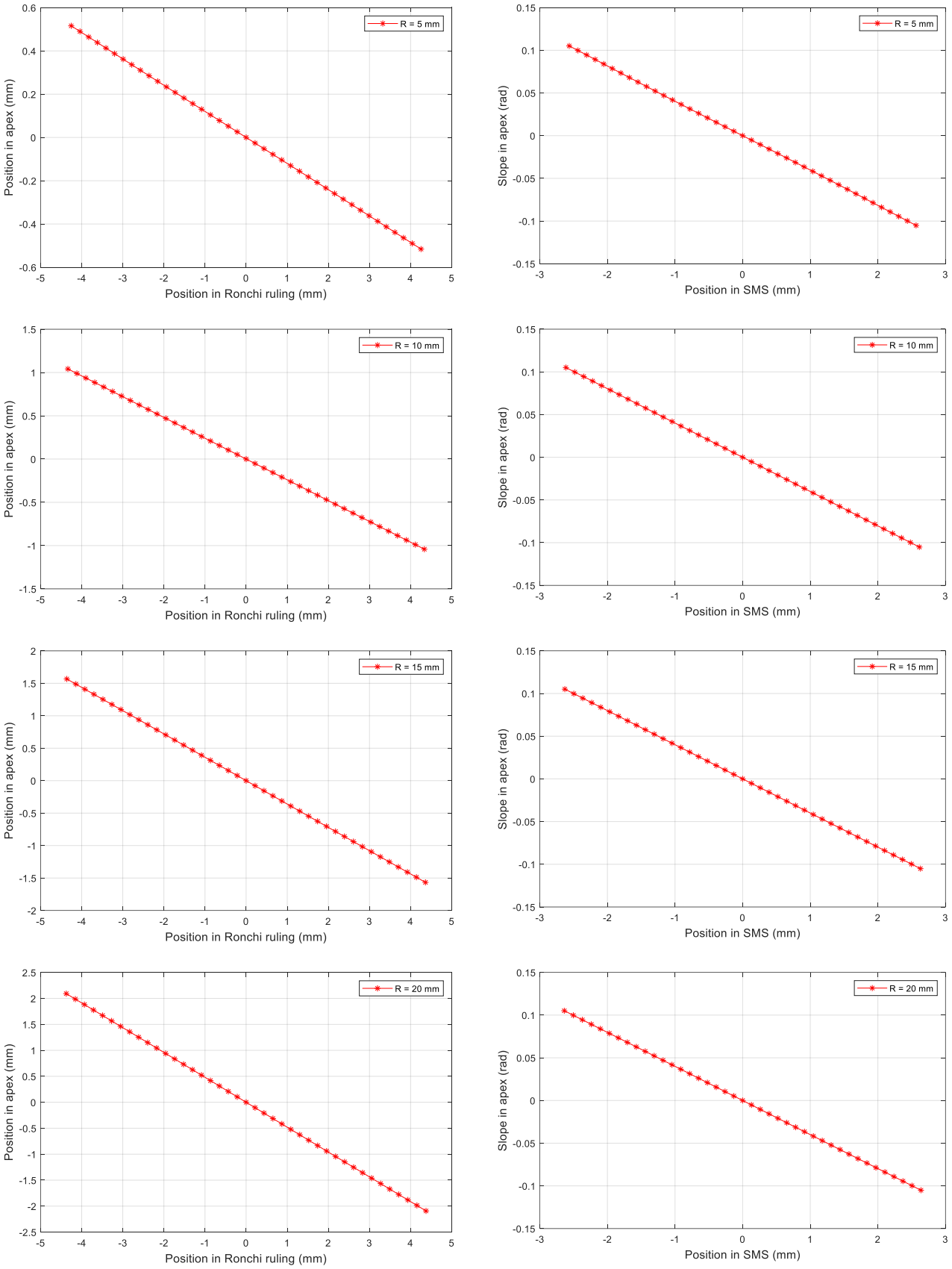

Fig 3 Graph representation of the relations needed to analyze the behavior of the divergence adapter in the measuring arm for the four radii analyzed. The graphs on the left represent the relation between the position in the Ronchi ruling plane and the position in the apex. The graphs on the right represent the relation between the position in the CMOS sensor plane of the SMS and the slope value in the apex.

 © Sociedad Española de Óptica

TABLE 1. The polynomial fit of the relations is shown in Fig. 3.

Radius (mm)	Position in the apex Vs. Position in Ronchi ruling	R^2	Slope in the apex Vs. Position in the CMOS sensor plane of the SMS	R^2
5	$Y = -0.120\ x - 1.21e^{-4}\ x^3 + 3.29e^{-6}\ x^5$	1	$Y = -0.0400\ x - 2.86e^{-4}\ x^3 + 2.18e^{-5}\ x^5$	1
10	$Y = -0.240\ x + 1.12e^{-5}\ x^3 - 1.78e^{-7}\ x^5$	1	$Y = -0.0402\ x - 5.28e^{-5}\ x^3 + 3.74e^{-6}\ x^5$	1
15	$Y = -0.361\ x + 1.35e^{-4}\ x^3 - 3.31e^{-6}\ x^5$	1	$Y = -0.0403\ x + 1.95e^{-5}\ x^3 - 1.48e^{-6}\ x^5$	1
20	$Y = -0.481\ x + 2.56e^{-4}\ x^3 - 6.37e^{-6}\ x^5$	1	$Y = -0.0403\ x + 5.47e^{-5}\ x^3 - 3.98e^{-6}\ x^5$	1

To do an equivalent analysis for the behavior of the divergence adapter in the illumination arm, we only need to find the relation between position and slope in the apex. A graph representation of these relations for the selected radii (5, 10, 15, and 20 mm) is shown in Fig. 4. For an easy treat, a polynomial fit of each relationship has been done and shown in table 2.

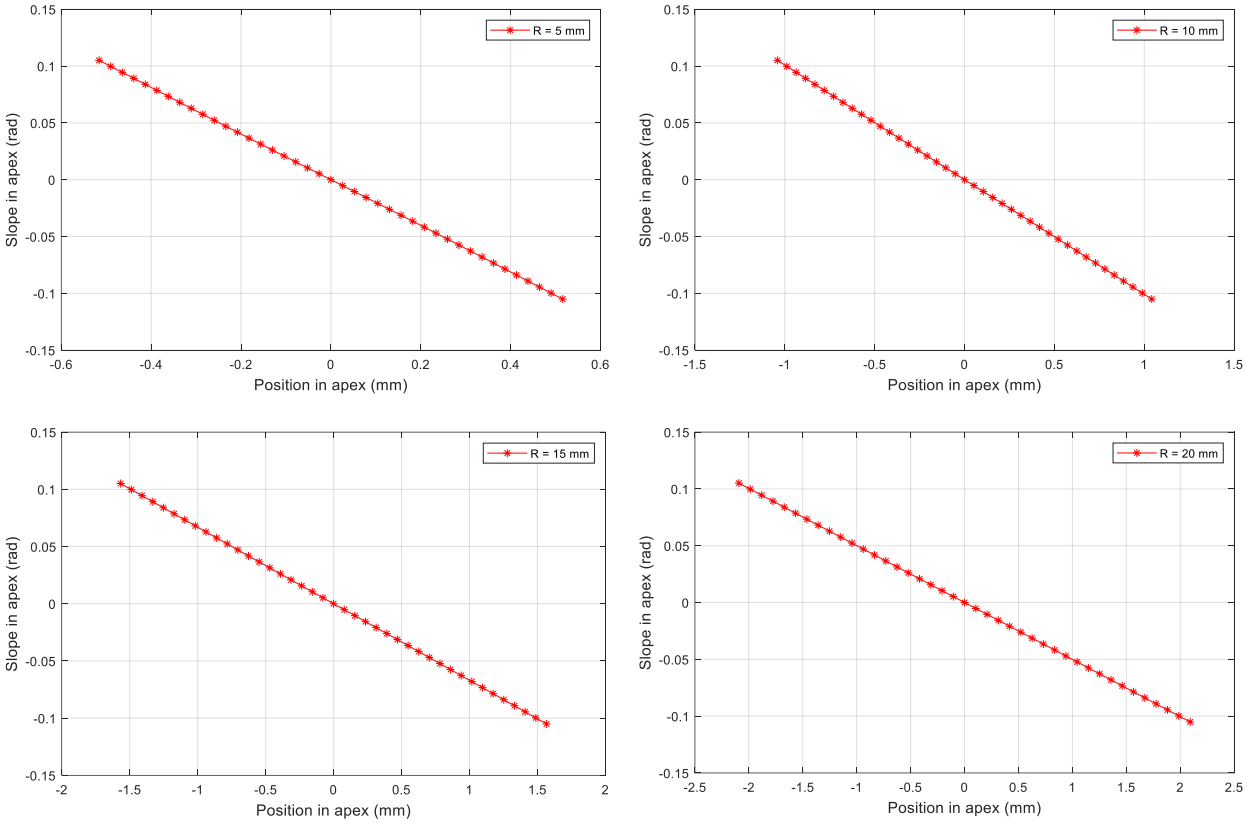

Fig. 4 Graph representation, position vs. slope in the apex, needed to analyze the behavior of the divergence adapter in the illumination arm for the four radii analyzed.

TABLE 2. The polynomial fit of the relations is shown in Fig. 4.

Radius (mm)	Slope Vs. Position in the apex	R^2
5	$Y = -0.199\ x - 2.77e^{-2}\ x^3 + 5.06e^{-2}\ x^5$	1
10	$Y = -0.0999\ x - 1.68e^{-3}\ x^3 + 7.60e^{-4}\ x^5$	1
15	$Y = -0.0667\ x - 3.29e^{-4}\ x^3 + 6.59e^{-5}\ x^5$	1
20	$Y = -0.0500\ x - 1.04e^{-4}\ x^3 + 1.17e^{-5}\ x^5$	1

By closely analyzing Fig. 3 (graphs on the right), we observe that the range of the abscissas and ordinates are the same for all four radii; this is a consequence of the design criteria used to build our Ronchi configuration. As we have decided to maintain the same dynamic range of SMS for all the cases, we have needed to place the curvature center of the convex surface near the light source image and the relation between the field sampling and the curvature radius becomes a constant. In Fig. 3 (graphs on the left), we observe that the range for the abscissas, position in the Ronchi ruling plane, is the same for all the radii, but

 © Sociedad Española de Óptica

the range in the ordinates changes because the position of the apex also changes. Finally, if we do the same analysis for the graphs in Fig. 4, we also observe that the slope range is the same for all the radii and the position ranges change from one case to another.

It is also interesting to observe that an odd fifth-order polynomic fit has been enough for all the graphs shown to adjust the simulated values. The polynomic fit does not have the independent term, the quadratic term is not present, and the importance of the third and fifth terms is lower than the linear term. The loss of the independent period was expected because all the systems were centered. The missing of the quadratic term was also expected because the light source is punctual, and only spherical aberration has relevance. Finally, the low values of the third and fifth terms tell us that design is closer to a paraxial design.

To answer whether the divergence adapters are good enough for our Ronchi deflectometry configuration, it is necessary to study in detail the sum of the third and fifth-order terms for all the radii and their corresponding threshold values.

4. Divergence adapter behavior

The divergence adapters have different functions; the divergence adapter of the measuring arm collects the light beam reflected in the surface, which will be sampled by the Ronchi ruling and the SMS, and the divergence adapter of the illumination arm conforms the light to be incident over the surface as close as possible in its local normal. However, the optical elements that are part of the divergence adapter, while shaping the light in the right path, introduce aberrations that disturb the wavefront and can disable its use in the selected Ronchi configuration.

The necessary information to answer if the divergence adapters are adequate for their use was obtained in the previous points. At point 2, “selected Ronchi configuration,” we have found that the threshold to ensure no confusion in the apex is 1/100 of the measuring field for positions and slopes. Those values were obtained through the chosen frequency of the Ronchi ruling and the size of the CMOS sensor used in the SMS. In point 3, “Optical simulations,” the simulation of the measuring arm provided the relations between sampling planes and the apex, and the simulation of the illumination arm provided the relations between the position-slope of the illumination beam in the apex.

To assure that, in the selected Ronchi configuration, the divergences adapters do not introduce errors between sampled neighbor values is necessary to know how far the relation is from linear behavior. When the relation is a linear one, the separation between sampled values is maintained along the measuring field, and as further as they get away from a linear fit as easier, the confusion between neighbor points becomes. In our strategy, as we have added a polynomial fit for each couple of data values, the difference between the real and the lineal behavior is directly quantified through the sum of the fitted polynomial's third and fifth-order terms in Fig. 5 and Fig. 6.

In Fig. 5 and Fig. 6, two dashed lines are shown on each graph. These lines mark the threshold of 1/100 of the measuring field, and the graph crosses the lines only in the case of a 5 mm radius. For the rest of analyzing configurations (radius 10, 15, and 20 mm), the graphs never cross the lines; so, in these cases, we can conclude that the aberrations introduced by the divergence’s adapters are low enough for the use of the divergence adapter in our Ronchi configuration.

 © Sociedad Española de Óptica

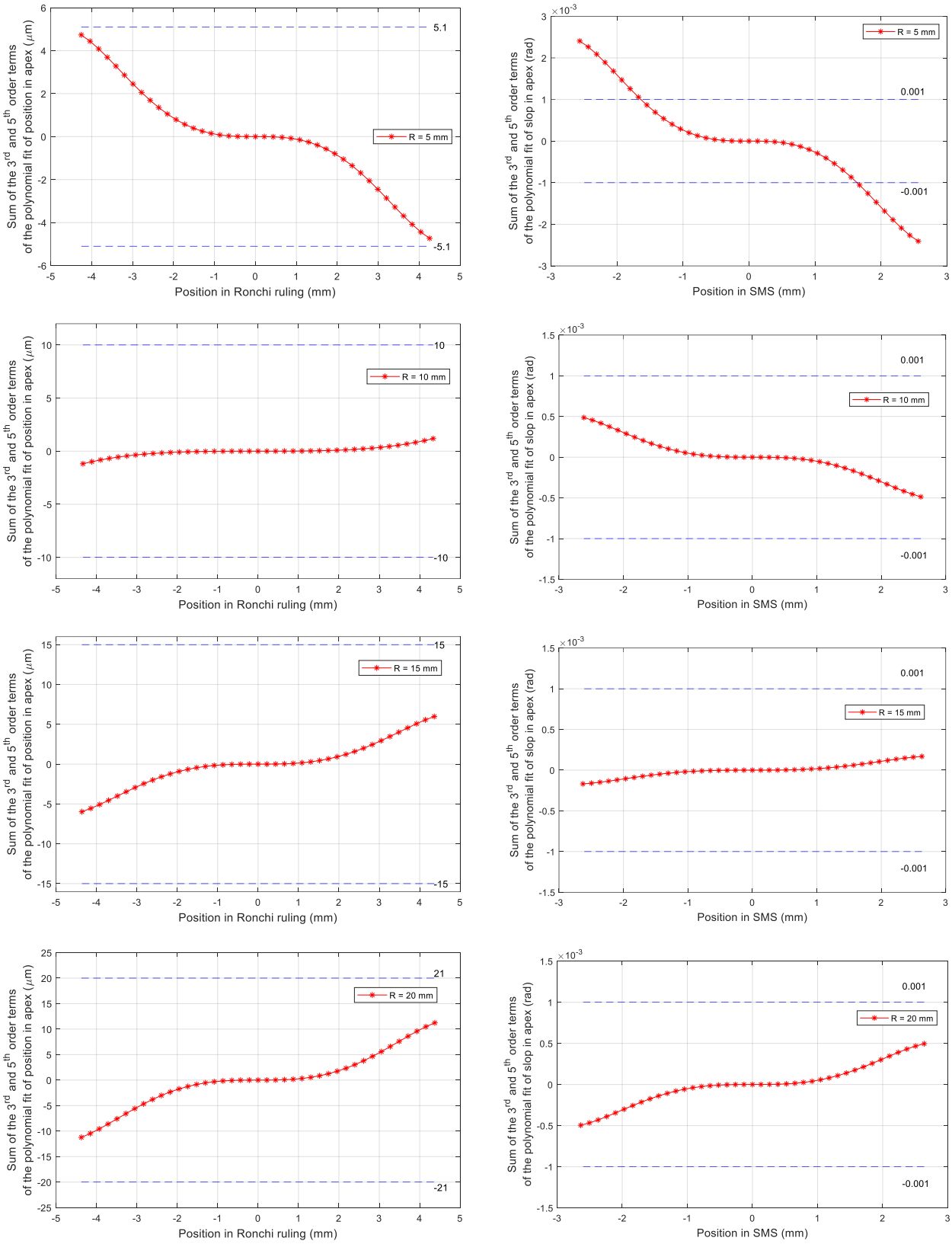

Fig. 5 Sum of third and fifth-order terms of the polynomial fit from the equations of table 1. The graphs on the left represent the relation between the position value in the Ronchi ruling plane and the position value in the apex. The graphs on the right represent the relation between the position value in the CMOS sensor plane of the SMS and the slope value in the apex. The horizontal dashed lines indicate the threshold value for each case.

 © Sociedad Española de Óptica

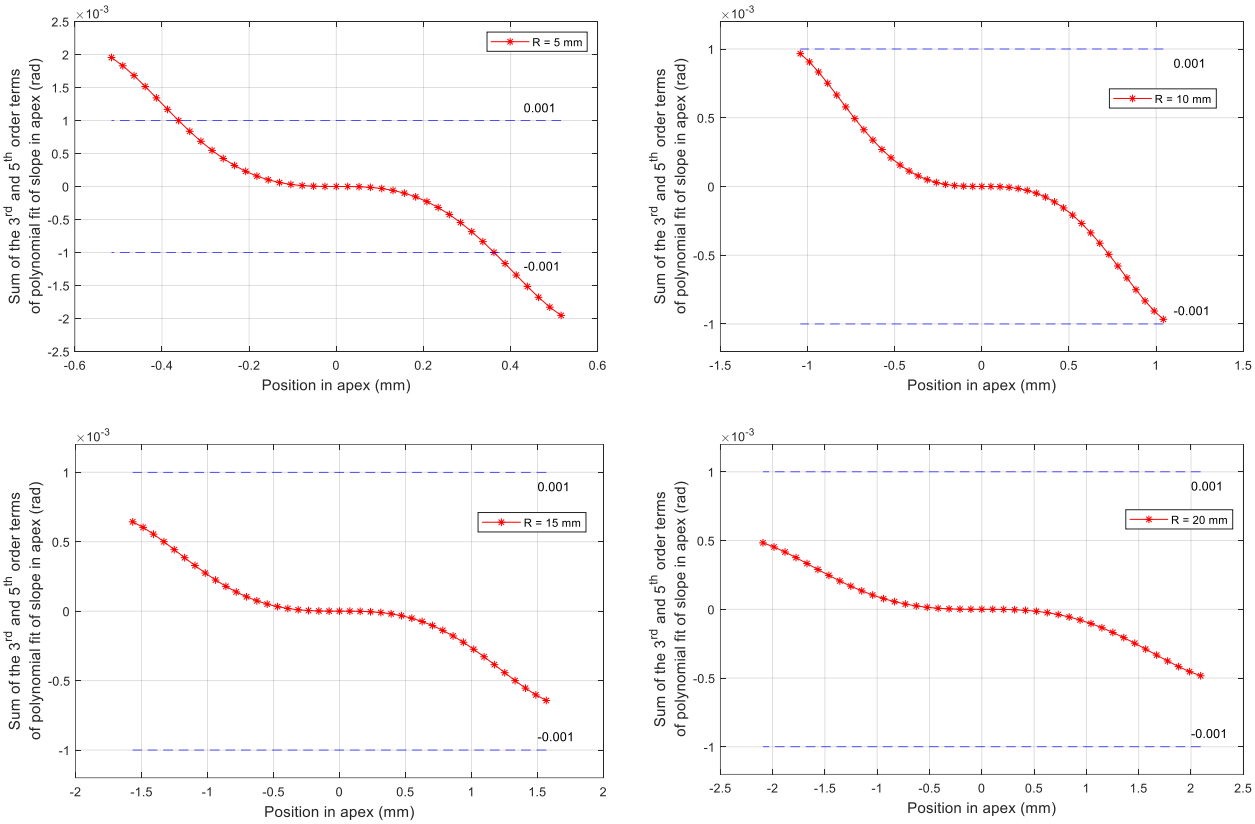

Fig. 6 Sum of third and fifth-order terms of the polynomial fit from the equations of table 2. The graphs show the relations between the position value and the slope value in the apex for the illumination arm and the four radii analyzed. The horizontal dashed lines indicate the threshold value for each case.

The case of a 5 mm radius needs a more detailed interpretation. Observing in detail graph 5 (graphs on the left), the relation between position in the Ronchi ruling and position at the apex does not have problems of confusion between neighbor points because the values remain under the threshold line. However, in graphs 5 (graphs on the right) and 6, only in the 50% of the measuring field do the values remain under the threshold, while in the other 50 %, near the borders, the values cross the line and reach a value of 1/33 the measuring field, three times, the value that, conservatively, we have fixed.

In this case, we can choose two different ways to overcome the problem, all acceptable. The first solution does not use 50% of the field near the border for samples of a 5 mm curvature radius. The second solution is to change the threshold value at 1/33 of the field; this solution needs a high accurate implementation in the building stage, but it is still possible to distinguish between two neighbor point values of slopes when the sampling period is 1/10 of the field and the resolution is 1/33 of the field. However, it is not a recommended solution if we want a robust experimental setup.

At this point, the main question has been answered; the divergence adapter, with the threshold set by the sampling elements, is appropriate for the proposed optical configuration whenever the interval of the surface radii to measure is constrained between 5 and 20 mm. The only partial exception was found in the case of a 5 mm radius for which only half of the field can be adequately measured. Furthermore, the same simulation process has provided information about the relations between sampling planes and the apex, see table 1, and between the position and slope for the illumination arm, see table 2, which is enough for an odd fifth-order polynomial fit for all the relations. One more step can be done by introducing an extra set of equations, including the radius variable, see table 3, to obtain the polynomial coefficients of tables 1 and 2.

 © Sociedad Española de Óptica

TABLE 3. Compact set of polynomial fit, including the radius (r) as a variable.

Position in the apex Vs. Position in Ronchi ruling	
$y = Ax + Bx^3 + Cx^5$	$A = 2.00e^{-4} - 2.40e^{-2}\ r$
	$B = -2.43e^{-4} + 2.51e^{-5}r$
	$C = 6{,}39e^{-6} - 6{,}42e^{-7}\ r$
Slope in the apex Vs. Position in the CMOS sensor plane of the SMS	
$y = A\ x + Bx^3 + Cx^5$	$A = -3.97e^{-2} - 7.00e^{-5}r + 2.00e^{-6}r^2$
	$B = -8.04e^{-4} + 1.40e^{-4}r - 8.17e^{-6}r^2 + 1.70e^{-7}r^3$
	$C = 6.28e^{-5} - 1.12e^{-5}r + 6.62e^{-7}r^2 - 1.30e^{-8}r^3$
Slope Vs. Position in the apex	
$y = A\ x + Bx^3 + Cx^5$	$A = -1.00(1/r)$
	$B = 1.23e^{-3} - 6.11e^{-2}(1/r) + 1.06(1/r)^2 - 7.38(1/r)^3$
	$C = -6.16e^{-3} + 2.85e^{-1}(1/r) - 4.32(1/r)^2 + 21.5(1/r)^3$

To summarize, the main divergence adapter functions are to conform the illumination beam that arrives at the convex surface to be near the local normal and make it easier for the reflected beams to pass through the Ronchi ruling and reach the CMOS sensor of the SMS. Those jobs must be done without confusion between neighboring sampled positions or slopes, and a transfer function can be written to describe the relations between sampling planes and the apex doing further data treatment in the Ronchi metrology strategy will be easier.

5. Conclusions

A method to analyze the optical behavior of the divergence adapter, necessary to be incorporated in a Ronchi deflectometry configuration to measure convex surfaces, has been presented. The analysis has been done following the following steps: First, the election of the desired Ronchi configuration. Second, identification of the elements and positions of the divergence adapters of the measuring and illumination arms. Third, obtaining the threshold values through the frequency of the Ronchi ruling and the number and size of the pixels of the SMS. Fourth is the selection of the radius interval desired to measure. Fifth, an individual simulation of each arm to obtain the relation between the position in the Ronchi ruling plane and the position in the apex, the position in the CMOS sensor and the slope in the apex, and the position and the slope in the apex for the illumination beam. Sixth, a fifth-order odd polynomic fit for the previous relations. Seventh and last, the application of the goodness criteria: The divergences adapters are adequate for a specific surface radius if the sum of the third and fifth-order term of the fitted polynomials remains under the threshold values in all the relations found relations and for all the measuring field. This criterion is equivalent to ensuring that the apex has not had problems of confusion, either of positions or slopes.

We have applied the above method to the divergence adapters used in the proposed Ronchi deflectometry setup for convex surfaces. We have found that they are suitable for measuring surfaces with radii from 5 to 20 mm; however, the required objective is not achieved in the case of a radius of 5 mm for half the measurement field.

To reach those results, the sampling elements have played a significant role. The first sampling element is the Ronchi ruling itself, with a frequency of $1 mm^{-1}$ and a field size of 10 mm has fixed the threshold for positions sampling in a 1/100 of the measuring field, assuming that is necessary, at least 1/10 of the ruling period to avoid identification errors. The same criteria have been applied to the second sampling element, the CMOS sensor; in this case, the threshold value is for the slope values and has been fixed in 1/100 of the measuring field, which is equivalent to the size of 10 pixels or ±0.00105 slope units. Finally, the same threshold value has been transferred to the illumination arm to ensure that an incorrect assignment between the position and slope of the incident beam no produces confusion between neighbor positions at the apex.

After determining the threshold values, each arm was simulated using OSLO™ software with a monochromatic and quasi-punctual light source. The simulation has provided three relations: position in Ronchi ruling vs. position at the apex, position in the CMOS sensor plane of the SMS vs. slope in the apex, and position vs. slope of the illumination beam in the apex. The graphs of the three relations are shown in Fig. 4 and Fig. 5, and an odd fifth-order polynomial has fitted. The sum of the third and fifth orders has been

 © Sociedad Española de Óptica

compared with the threshold values in the entire measuring field, finding that in none of the field positions the value crosses the threshold, except for the 5 mm radius, where only half of the field remains below the threshold. In the case of a 5 mm radius, the 50% of the field near the border reaches a value of 3 times the threshold keeping away an easy way to distinguish between two neighbors' values of slopes.

A complete description of the three sets of polynomial fits has been included introducing the radius of curvature of the surface as a variable. This more compact writing, shown in table 3, will be helpful when we are interested to know the transfer functions for a no-simulated radius of curvature, however, do not provide information about the goodness of the divergence adaptors because neither the sampling elements nor the thresholds are included.

 © Sociedad Española de Óptica